Proceedings of the ASME 2013 Summer Heat Transfer Conference
SAND2013-4089C
HT2013
July 14-19, 2013, Minneapolis, MN

HT2013-17541

THE EFFECT OF BALLISTIC ELECTRON TRANSPORT ON COPPER-NIOBIUM THERMAL INTERFACE CONDUCTANCE

Ramez Cheaito
University of Virginia
Charlottesville, VA 22904, USA

John C. Duda
University of Virginia
Charlottesville, VA 22904, USA

Thomas E. Beechem
Sandia National Laboratories
Albuquerque, NM 87123, USA

Douglas L. Medlin
Sandia National Laboratories
Livermore, CA 94550, USA

Khalid Hattar
Sandia National Laboratories
Albuquerque, NM 87123, USA

Edward S. Piekos
Sandia National Laboratories
Albuquerque, NM 87123, USA

Amit Misra
Los Alamos National Laboratory
Los Alamos, NM 87545, USA

Jon K. Baldwin
Los Alamos National Laboratory
Los Alamos, NM 87545, USA

Patrick E. Hopkins*
University of Virginia
Charlottesville, VA 22904, USA

ABSTRACT
The thermal conductivities of 1μm copper-niobium multilayer films of different period thicknesses are measured by time–domain thermoreflectance at room temperature. The values for thermal conductivity are then used to calculate the thermal conductance between Cu/Nb interfaces using a series resistors model. Results show that Cu/Nb interface conductance increases with the decrease in period thickness reaching a value as high as 20 $GWm^{-2}K^{-1}$ for a 1x1 Cu/Nb multilayer. At shorter period thicknesses, ballistic electron transport dominates the thermal transport across this interface resulting in high interface conductance. The results are well described by a model that accounts for both ballistic and diffusive transport of electrons. This model assumes that an electron on one side of a metal-metal multilayer may not scatter at the interface but rather move ballistically on to the adjacent material and scatter in the adjacent material.

INTRODUCTION
Thermal transport across interfaces has been studied intensively over the past two decades. As the size of electronic devices decreases, transport across interfaces becomes a critical consideration and thermal management becomes a challenging issue [1]. Most of previous studies focused on phonon mediated material systems [2,3] and much less attention was given to transport across metal-metal interfaces [4]. Metal multilayers have recently gained more attention due to their use in magnetic applications [5] and the discovery of giant magnetoresistance effect (GMR) in metal multilayers [6]. Nevertheless, research in the domain of thermal transport across metal multilayers has been very limited and very few metallic multilayer systems have been investigated [7–10]. Clemens, Easley and Paddock [7] utilized picosecond time-resolved thermoreflectance measurements and investigated the effect of the interface on thermal transport across Ni-Cu , Ni-Mo, Ni-Ti, and Ni-Zr metallic multilayers. Soe *et al.* [8] showed that Wiedmann Franz law holds in Ag/Al and Ag/Cu multilayers. Yang *et al.*[9] measured the electrical and thermal conductivities of Cu/CoFe and reported on the GMR of these multilayers. Wilson and Cahill [10] have recently performed thermal conductivity measurements on Pd/Ir metal multilayers to experimentally validate Wiedman-Franz law at these metal interfaces. Traditionally, conduction electrons that are well known to be

* Author to whom correspondence should be addressed phopkins@virginia.edu

the dominant heat carriers in these structures are treated diffusively [4,10–13]. This treatment arises primarily from the assumption that electrons are non-spectral and a single mean free path is enough to describe electronic transport.

In this work, we measure the thermal conductivity of four 1µm thick copper-niobium metallic multilayers of 2, 10, 20 and 100 nm period thicknesses. We observe a strong dependence of thermal conductivity on period thickness. This dependence can not be explained by the electronic version of the diffuse mismatch model (EDMM) as previously reported [10,12]. In this paper we show that at very low period thicknesses electrons can behave ballistically giving rise to interface conductances as high as 20 GWm^{-2}K^{-1}.

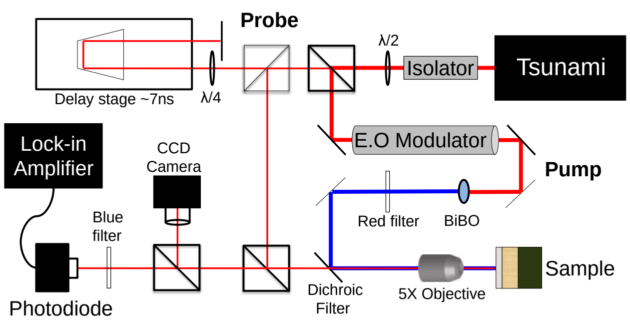

Figure 1 A schematic representation of the pump-probe experiment used to measure the thermal conductivity of Cu-Nb multilayers.

SAMPLES

Cu-Nb multilayer films were synthesized by means of DC magnetron sputtering at room temperature on Si substrates. The deposition was carried at 4 mTorr argon partial pressure with a deposition rate of ≈ 0.6 nm/s. The copper and niobium targets were 100 mm in diameter and were held at powers of 100 W and 200 W, respectively. The films have a columnar grain structure with a strong fiber texture {111}Cu/{110}Nb/interface plane, and Kurdjumov-Sachs orientation relationship {110}Nb/{111}Cu, and <111>Nb/<110>Cu.

EXPERIMET

We measure the thermal conductivity of our samples with time domain thermoreflectance (TDTR)[14][15]. TDTR is a pump-probe technique in which the laser output of a mode-locked Ti:Sapphire oscillator is split into two paths: a pump and probe. A schematic of the key elements in our experiment is shown in figure 1. In our setup, the laser operates at 80 MHz repetition rate with pulses centered at 800 nm and pulse widths of 150 fs. The pump path is modulated with an electro-optic modulator driven by a sinusoidal modulation waveform at a frequency of 11.4 MHz. The pump then undergoes a second harmonic generation in a BIBO crystal that converts the 800 nm light to 400 nm. A mechanical delay stage is used to delay the arrival of the probe to the sample surface with respect to the pump. The stage gives time delays up to 7 ns. The pump and probe beams are then coaxially focused by a microscope objective to roughly 24.5 μm and 6 μm radii at the sample surface, respectively. The microscope objective can be used to view the image of the sample on a CCD camera. The reflected probe is directed to a photodetector connected to the lock-in amplifier. Because of the periodic heating created by pump modulation on the sample surface, the reflected probe contains a frequency component at the pump modulation, which also acts as a reference frequency to the lock-in amplifier. We use the ratio of the in-phase and out-of-phase components of the thermoreflectance signal detected by the lock-in amplifier to monitor the surface temperature decay over the full time delay range. Prior to TDTR measurements, we coat the samples with a thin aluminum film that acts as temperature transducer. We measure the thickness of the Al films during each measurement with picosecond ultrasonics [16,17]. We assume literature values for the heat capacity and thermal conductivity of the Al film and the silicon substrate. We treat the Cu-Nb multilayers as one layer of 1μm thickness and use a weighted average of the bulk heat capacity values of Cu and Nb. We set the interface conductance between the Cu-Nb film and the silicon substrate to infinity, although we are not sensitive at all to this parameter given the large thickness of the Cu-Nb film and the high modulation frequency used in our experiment. Hence the only unknowns in our thermal model are the Al/Cu-Nb Kapitza conductance and the thermal conductivity of the Cu-Nb film. These parameters are treated as free parameters and are varied to fit the data to a multilayer thermal model that has been detailed by many groups elsewhere [18–20]. Figure 2 shows a sample data and best fit curve for the 1x1 Cu-Nb sample.

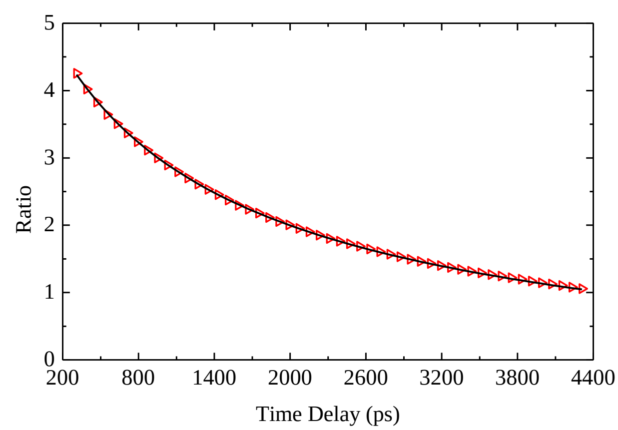

Figure 2 TDTR data and best fit curves for the 1x1 Cu-Nb sample. The best fit value for thermal conductivity for this data set is 17.1 Wm^{-1}K^{-1}.

MODEL AND DISCUSSION

The results for the thermal conductivity measurements as a function of period thickness on the four different samples are shown in Figure 3. The interface conductance is inferred from these thermal conductivity measurements using a series resistor model similar to Wilson and Cahill [10]. The total thermal resistance of the Cu-Nb film is thus given by:

$$R_{tot} = \frac{t}{k_{measured}} = R_o + \frac{n}{h_{Cu/Nb}} \tag{1}$$

with:

$$R_o = \frac{t}{2\kappa_{Cu(bulk)}} + \frac{t}{2\kappa_{Nb(bulk)}} \tag{2}$$

Where t is the thickness of the Cu-Nb sample which is 1 μm for all the samples, n is the number of interfaces, h is the interface conductance between the copper and niobium layers, κ is the thermal conductivity, R_o is the thermal resistance of the sample without the interfaces. The interface conductance between the copper and niobium multilayers are shown in figure 4. The data shows an increase in interface conductance at shorter periods.

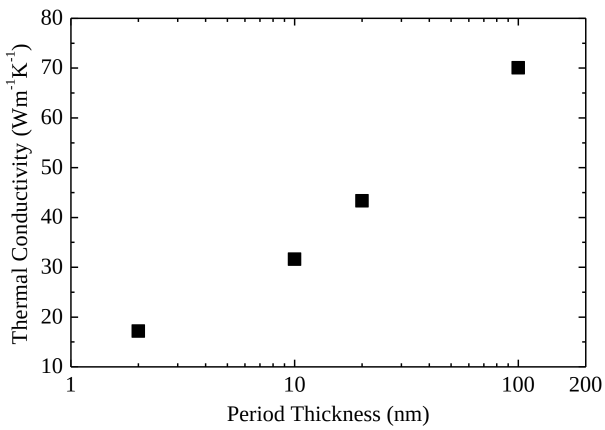

Figure 3 The thermal conductivity as function of period thickness for the four Cu-Nb samples, 1x1, 5x5, 10x10, and 50x50.

To gain a quantitative understanding of these results we suggest the following model. Electrons on the copper side can be well described by the free electron model. Having a relatively long mean free path, they move ballistically from the copper side to the niobium side where they scatter diffusively. The thermal interface conductance is thus the sum of the contribution of both the electrons ballistically crossing the Cu-Nb interface and those diffusively scattering in Niobium. Thus:

$$h = h_{ballistic}\beta + h_{diffusive}(1-\beta) \tag{3}$$

Where $\beta = \exp(-d/\lambda)$ is a term derived from ballistic diffusive equations [21] and gives the exponential decay of heat flux across interface, d is half the period thickness, and λ is an effective mean free path (see Appendix B), which we estimate as

$$\frac{1}{\lambda} = \frac{1}{\lambda_{Cu}} + \frac{1}{\lambda_{Nb}} \tag{4}$$

The diffusive part of the interface conductance follows the EDMM as given by Gundrum *et al.*[12]:

$$h_{Diffusive} = \frac{1}{4}\zeta_{1\to2} C_{e,Cu} \upsilon_{F,Cu} \tag{5}$$

Where

$$\zeta_{1\to2} = \frac{D(\varepsilon_{F,Nb})\upsilon_{F,Nb}}{D(\varepsilon_{F,Nb})\upsilon_{F,Nb} + D(\varepsilon_{F,Cu})\upsilon_{F,Cu}} \tag{6}$$

The ballistic component is simply the temperature derivative of the heat flux through the Cu.

$$h_{ballistic} = \frac{1}{4} C_{e,Cu} u_{F,Cu} \tag{7}$$

All the material properties are given in Table I, and model details are given in the Appendix.

Table I. Material properties for Copper and Niobium

Material	Property	Value	Reference
Cu	$D(\varepsilon_F)$	1.134×10^{47} m^{-3}	[22]
	ε_F	7 eV	[22]
	υ_F	1.57×10^{6} m s^{-1}	[22]
	λ	35 nm	see Appendix B
Nb	$D(\varepsilon_F)$	5.4×10^{47} m^{-3}	[23]
	υ_F	6.48×10^{5} m s^{-1}	see Appendix A
	λ	1.7 nm	see Appendix B

We normalize the ballistic part of the model with the data point for the 1×1 (d = 1 nm) multilayer. Figure 4 shows both the ballistic and diffusive contributions to the total interface conductance. The general trends that we observe in Cu/Nb interface conductance show a decrease as the period thickness is increased. This is correctly captured in our ballistic-diffusive calculations of h, indicating an exponentially decreasing ballistic electron flux in the Cu layers.

In contrary to our findings, Wilson and Cahill found that the interface conductance in Pd/Ir multilayers is independent of the period thickness and were able to explain the result by EDMM. We attribute this to fact that the mean free path of electrons in copper is large compared to that of palladium and iridium. As a result, these long mean free path electrons contribute to the ballistic transport at short period thicknesses.

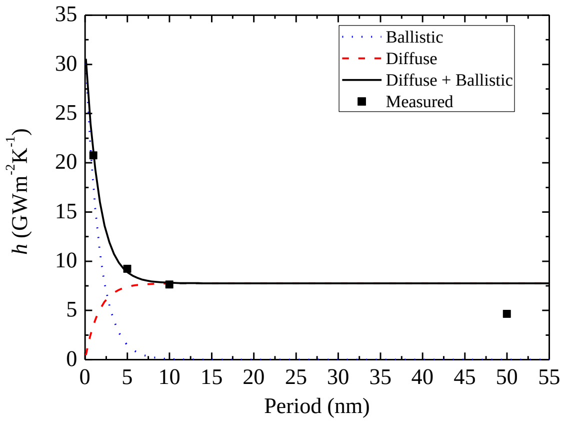

Figure 4 Data and model for the interface conductance between copper and niobium interfaces. The figure shows both ballistic and diffusive portions of the model. Note that the x-axis represents half the period thickness of the multilayer.

CONCLUSION

We presented data on thermal interface conductance in Cu/Nb multilayers. The data showed an increase in interface conductance with the decrease in period thickness. The results are well described by a model that accounts for both ballistic and diffusive transport of electrons. Long mean free path electrons originating at the copper side ballistically cross the interface causing an increase in interface conductance in short period thicknesses. Future work will include performing the same measurements and calculations on the same samples at low and high temperatures.

NOMENCLATURE

ε_F = Fermi energy
$D(\varepsilon_F)$ = density of states at the Fermi level in m^{-3}
C_e = electronic heat capacity in $Jm^{-3}K$
υ_F = Fermi velocity in ms^{-1}
λ = mean free path
$\zeta_{1\rightarrow 2}$ = transmission probability

ACKNOWLEDGMENTS

This work was performed in part at the Center for Atomic, Molecular, and Optical Science (CAMOS) at the University of Virginia. We are appreciative of funding through the Laboratory Directed Research and Development program at Sandia National Laboratories. Sandia National Laboratories is a multiprogram laboratory managed and operated by Sandia Corporation, a wholly owned subsidiary of Lockheed Martin Corporation, for the U.S. Department of Energy National Nuclear Security Administration under Contract No. DE-AC04-94AL85000. P. E. H. and J. C.D are appreciative for support from NSF Grant No. CBET 1134311. A. M and J. K. B at LANL acknowledge support from DOE, Office of Science, and Office of Basic Energy Sciences.

REFERENCES

[1] Cahill D. G., Ford W. K., Goodson K. E., Mahan G. D., Majumdar A., Maris H. J., Merlin R., and Phillpot S. R., 2003, “Nanoscale thermal transport,” Journal of Applied Physics, **93**(2), p. 793.

[2] Swartz E., and Pohl R., 1989, “Thermal boundary resistance,” Reviews of Modern Physics, **61**(3), pp. 605–668.

[3] Little W. A., 1959, “The Transport of Heat between Dissimilar Solids at Low Temperatures,” Canadian Journal of Physics, **37**(3), pp. 334–349.

[4] Pratt W. P., and Bass J., 2009, “Perpendicular-current studies of electron transport across metal/metal interfaces,” Applied Surface Science, **256**(2), pp. 399–403.

[5] McDaniel T. W., 2005, “Ultimate limits to thermally assisted magnetic recording,” Journal of Physics: Condensed Matter, **17**(7), pp. R315–R332.

[6] Baibich M. N., Broto J. M., Fert A., Nguyen Van Dau F., and Oetroff F., 1988, “Fel(001),” Physical Review Letters, **61**(001), pp. 2472–2475.

[7] Clemens B. M., Eesley G. L., and Paddock C. A., 1988, “Time-resolved thermal,” **37**(3).

[8] Soe W., 1993, “Measurements of transport properties of Ag / A1 and Ag / Cu multilayered films,” **126**, pp. 457–459.

[9] Yang Y., Zhu J.-G., White R. M., and Asheghi M., 2006, “Field-dependent thermal and electrical transports in Cu⁄CoFe multilayer,” Journal of Applied Physics, **99**(6), p. 063703.

[10] Wilson R., and Cahill D., 2012, “Experimental Validation of the Interfacial Form of the Wiedemann-Franz Law,” Physical Review Letters, **108**(25), p. 255901.

[11] Shpiro A., and Levy P., 2000, “Resistance across an interface, and that measured far from it,” Physical Review B, **63**(1), p. 014419.

[12] Gundrum B., Cahill D., and Averback R., 2005, “Thermal conductance of metal-metal interfaces,” Physical Review B, **72**(24), pp. 1–5.

[13] Bauer G. E. W., Schep K. M., Xia K., and Kelly P. J., 2002, “Scattering theory of interface resistance in magnetic multilayers,” **2410**.

[14] Cahill D. G., Goodson K., and Majumdar A., 2002, “Thermometry and Thermal Transport in Micro/Nanoscale Solid-State Devices and Structures,” Journal of Heat Transfer, **124**(2), p. 223.

[15] Hopkins P. E., Serrano J. R., Phinney L. M., Kearney S. P., Grasser T. W., and Harris C. T., 2010, “Criteria for Cross-Plane Dominated Thermal Transport in Multilayer Thin Film Systems During Modulated Laser Heating,” Journal of Heat Transfer, **132**(8), p. 081302.

[16] C. Thomsen, J. Strait, Z. Vardeny, H. J. Maris J. T., 1984, “Coherent Phonon Generation and Detection by Picosecond Light Pulses,” Physical review letters, **53**(10), p. 989.

[17] C. Thomsen, H. T. Grahn, H. J. Maris J. T., 1986, “Surface generation and detection of phonons by picosecond light pulses,” Physical Review B, **34**(6), p. 4129.

[18] Cahill D. G., 2004, “Analysis of heat flow in layered structures for time-domain thermoreflectance,” Review of Scientific Instruments, **75**(12), p. 5119.

[19] Schmidt A. J., Chen X., and Chen G., 2008, “Pulse accumulation, radial heat conduction, and anisotropic thermal conductivity in pump-probe transient thermoreflectance.,” The Review of scientific instruments, **79**(11), p. 114902.

[20] Hopkins P. E., Serrano J. R., Phinney L. M., Kearney S. P., Grasser T. W., and Harris C. T., 2010, “Criteria for Cross-Plane Dominated Thermal Transport in Multilayer Thin Film Systems During Modulated Laser Heating,” Journal of Heat Transfer, **132**(8), p. 081302.

[21] Chen G., 2001, “Ballistic-Diffusive Heat-Conduction Equations,” Physical Review Letters, **86**(11), pp. 2297–2300.

[22] Kittle C., 2004, Introduction to Solid State Physics, Wiley.

[23] Jani A. R., Brener N. E., and Callaway J., 1988, “Band structure and related propeties of bcc niobium,” Physical Review B, **38**(14), pp. 9425–9433.

[24] Belmiloudi A., 2011, Heat Transfer- Mathematical Modelling , Numerical Methods and Information.

APPENDIX A
NIOBIUM FERMI VELOCITY

The niobium Fermi velocity is deduced from the ratio of free electron model density of states to that of the numerical value of density of state at Fermi level given in ref [23]:

$$\frac{D(\varepsilon_{F,Nb})}{D(\varepsilon_{F,Nb,free})} = \frac{\varepsilon_{F,Nb}^{1/2}}{\varepsilon_{F,Nb,free}^{1/2}} = \frac{5.4\times10^{47}}{1.14\times10^{48}} = 0.47$$

$$\frac{\upsilon_{F,Nb}}{\upsilon_{F,Nb,free}} = 0.47$$

$$\upsilon_{F,Nb} = 6.48\times10^{5}\, m/s$$

with $\upsilon_{F,Nb,free} = 1.37\times10^{6} ms^{-1}$ taken from [22]

APPENDIX B
MEAN FREE PATH CALCULATION

The effective mean free path is estimated by: $\frac{1}{\lambda} = \frac{1}{\lambda_{Cu}} + \frac{1}{\lambda_{Nb}}$

The mean free paths of copper and niobium are deduced from temperature dependent bulk thermal conductivity values. The thermal conductivity of a metal is given by [24]:

$$\kappa = \frac{\pi^2 k_B^2 N \upsilon_F^2}{6\varepsilon_F (A_{ee}T + B_{ep})}$$

A_{ee} and B_{ep} are determined by non-linear regression and used to calculate the mean free path:

$$\lambda = \upsilon_F \tau = \frac{\upsilon_F}{A_{ee}T^2 + B_{ep}T}$$